Evaluation of the Inhomogeneous Granular Sludge Distribution inside an Industrial-Scale Anaerobic Wastewater Treatment Reactor Using a Three-Phase Flow Model

Tarworn Ruttithiwapanich[1], Wimolsiri Pridasawas[2], Wiwat Ruenglertpanyakul[3]

King Mongkut's University of Technology Thonburi, Bangmod, Thungkru, Bangkok 10140

and Warinthorn Songkasiri[4*]

National Center for Genetic Engineering and Biotechnology, Bangkhuntien, Bangkok 10150

Abstract

An anaerobic fixed film reactor (AFFR) was designed and installed in a cassava starch factory in the east of Thailand to treat high-strength organic wastewater. Upon measuring the total suspended solids and soluble COD in the AFFR to investigate the granular sludge and substrate distribution inside the reactor, respectively, insufficient degree of mixing was noted. This research then attempted to use a three-phase flow model to investigate the effects of the inlet distribution on the granular sludge distribution inside the reactor; multiphase Eulerian-Eulerian modeling approach along with the k-ε turbulence model was used. The simulation showed that the inlet orifices adjacent to the reactor wall accelerated the liquid up-flow velocity to be higher than the sludge's terminal velocity of 0.0276 m/s, and so encouraged granular sludge floatation. When a homogeneous inlet distribution was applied, granular sludge floatation mainly occurred in the sludge-bed, where the inlet pipe was located. The inlet distribution design is a key factor in defining the granular sludge distribution in an AFFR. Understanding the flow behavior of the individual phases (liquid, solid and gas) is of benefit in designing high mixing efficiency reactors.

Keywords : Anaerobic Digestion / Biogas / CFD / Mixing / Wastewater Treatment

* *Corresponding Author : warinthorn@biotec.or.th*

[1] *Ph.D. Candidate, Department of Chemical Engineering, Faculty of Engineering.*

[2] *Assistant Professor, Department of Chemical Engineering, Faculty of Engineering.*

[3] *Associate Professor, Department of Chemical Engineering, Faculty of Engineering.*

[4] *Principle Lecturer, Excellent Center for Waste Utilization Management (ECoWaste).*

การกระจายตัวของเม็ดตะกอนภายในถังปฏิกรณ์บำบัดน้ำเสียแบบไร้อากาศขนาดโรงงานอุตสาหกรรมด้วยแบบจำลองสามสถานะ

ถาวร รัตติทิวาพาณิชย์[1] วิมลศิริ ปรีดาสวัสดิ์[2] วิวัฒน์ เรืองเลิศปัญญากุล[3]
มหาวิทยาลัยเทคโนโลยีพระจอมเกล้าธนบุรี บางมด ทุ่งครุ กรุงเทพฯ 10140
และ วรินธร สงคศิริ[4*]
ศูนย์พันธุวิศวกรรมและเทคโนโลยีชีวภาพแห่งชาติ บางขุนเทียน กรุงเทพฯ 10150

บทคัดย่อ

จากการศึกษาระบบผลิตก๊าซชีวภาพชนิดตรึงฟิล์ม (anaerobic fixed film reactor - AFFR) ซึ่งได้รับการออกแบบและติดตั้งที่โรงงานผลิตแป้งมันสำปะหลังแห่งหนึ่งในภาคตะวันออกของประเทศไทยให้สามารถรองรับน้ำเสียที่มีความเข้มข้นของสารอินทรีย์สูง โดยการวัดค่าของแข็งแขวนลอยและปริมาณของออกซิเจนทั้งหมดที่ต้องใช้เพื่อทำปฏิกิริยาเคมีกับสารอินทรีย์ที่ละลายอยู่ในน้ำภายในถังปฏิกรณ์ พบว่ามีการกวนผสมที่ไม่ทั่วถึง งานวิจัยนี้จึงใช้แบบจำลองการไหลแบบสามวัฏภาคเพื่อศึกษาอิทธิพลของทางน้ำขาเข้าที่มีต่อการกระจายตัวของเม็ดตะกอนภายในถังปฏิกรณ์ผลิตก๊าซชีวภาพชนิดตรึงฟิล์ม ด้วยวิธีการแบบ Eulerian-Eulerian และใช้แบบจำลองความปั่นป่วนแบบ k-ε model พบว่ารูกระจายน้ำเสียขาเข้าที่บริเวณใกล้ผนังของถังปฏิกรณ์เร่งความเร็วไหลขึ้นของน้ำเสียภายในถังจนมีค่าสูงกว่าความเร็วการตกอิสระของเม็ดตะกอนที่มีค่าเท่ากับ 0.0276 m/s จึงเร่งเม็ดตะกอนให้ลอยตัวเฉพาะในบริเวณดังกล่าว และเมื่อจำลองการไหลภายใต้สภาวะที่น้ำเสียขาเข้าเกิดการกระจายตัวอย่างทั่วถึง พบการลอยตัวของเม็ดตะกอนขนาด 2 mm เฉพาะภายในชั้น sludge-bed ซึ่งเป็นบริเวณที่ติดตั้งท่อกระจายน้ำเสียขาเข้า ความเข้าใจการพฤติกรรมขององค์ประกอบแต่ละวัฏภาค เช่น ของเหลว ของแข็ง และก๊าซนี้จะเป็นประโยชน์ต่อการออกแบบถังปฏิกรณ์ที่มีประสิทธิภาพการกวนผสมสูงต่อไป

คำสำคัญ : กระบวนการย่อยสลายแบบไม่ใช้อากาศ / ก๊าซชีวภาพ / การคำนวณพลศาสตร์ของไหล / การกวนผสม / การบำบัดน้ำเสีย

* *Corresponding Author : warinthorn@biotec.or.th*

[1] *นักศึกษาระดับปริญญาเอก ภาควิชาวิศวกรรมเคมี คณะวิศวกรรมศาสตร์*

[2] *ผู้ช่วยศาสตราจารย์ ภาควิชาวิศวกรรมเคมี คณะวิศวกรรมศาสตร์*

[3] *รองศาสตราจารย์ ภาควิชาวิศวกรรมเคมี คณะวิศวกรรมศาสตร์*

[4] *อาจารย์ ศูนย์ความเป็นเลิศเฉพาะทางด้านการจัดการและใช้ประโยชน์จากของเสียอุตสาหกรรมการเกษตร*

1. INTRODUCTION

Biogas production technology was introduced in Thailand in the 1960s [1]. During 1995 to 2006, more than 2,300 biogas plants were built around the country [2], of which 70% were anaerobic fixed dome reactors and the rest were the more advanced technologies of 189 upflow anaerobic sludge blanket (UASB) plants, nine anaerobic fixed film reactor (AFFR) plants, eight continuous stirred tank reactors and six anaerobic baffled reactor (ABR) plants [2]. Cassava starch factories in Thailand mostly use advanced biogas production technologies, such as UASB, AFFR, ABR and anaerobic hybrid reactor (AHR) to treat their wastewater and recover energy [1, 2].

Reactors with a hydraulic upflow pattern have been chosen for operating several biogas production technologies (UASB, AFFR, internal circulation, expanded granular sludge blanket and AHR). The hydraulic upflow pattern is beneficial for the formation of a compact granular sludge [3], which is known to provide a better performance of organic degradation and biogas production [4-6].

Biogas production depends on the microbial activity, reactor operating condition, reactor design and level of mixing between the phases, especially the microbes and substrates [7]. Mixing facilitates microbe-substrate encounters [7], but enhancing the level of mixing in an industrial-scale upflow reactor is a challenging task since its volume can be as high as 6,000 m^3. In such a large system, improper mixing easily occurs because of the complex interactions among the wastewater, granular sludge and biogas bubbles. The appearance of a compact layer of granular sludge, as the sludge bed, on the reactor's floor increases the resistance to the inertial mixing force, where the sludge bed reduces the mixing degree between the inlet wastewater and granular sludge in the reactor [8]. This work used a three-phase flow model to investigate the effects of the inlet distribution on the granular sludge distribution inside an AFFR. The operating conditions of the cassava starch factory AFFR were used as a case study. The total suspended solid (TSS) and soluble chemical oxygen demand (sCOD) were measured to investigate the granular sludge and substrate distribution inside the reactor. An understanding of the effect of the inlet and reactor designs on the granular sludge distribution will be useful for enhancing the granular sludge floatation, which increases the mixing efficiency between the sludge and wastewater within the sludge bed [9].

2. EXPERIMENTAL SET-UP AND PROCEDURES

Upflow AFFR for cassava wastewater treatment

Monitoring of the actual TSS and sCOD profiles, and the three-phase flow simulation using computational fluid dynamics (CFD), were performed in the industrial scale AFFR of a native cassava starch factory in eastern Thailand, as shown in Figure 1. This reactor has been operating for more than 15 y with a working volume of 4,750 m^3 and an operational inlet feeding rate of 1,200 m^3/d through four inlet distribution pipes. In each pipe, the inlet wastewater was fed from both ends and was distributed into the reactor through 61 nozzles along the length of the pipe.

Figure 1 The AFFR of the cassava starch factory.

Solid and substrate distribution inside the AFFR

Twenty-four samples of granular sludge were collected from four sampling ports located at the top of the reactor. Each sampling port represented the condition within a quarter of the reactor's volume (quarters I, II, III and IV). At each sampling port, sludge was collected at a height of 0, 1, 2, 3, 4 and 5 m. The TSS and sCOD of each sample was measured, which represents the distribution of sludge granules and substrate, respectively, inside the reactor. For the TSS analysis, 10 mL of sample suspension was filtered through a glass fiber filter (Schleicher & Schuell GF52, 1-1.2 μm) and the filtrate was then incubated in a hot air ovenat 105°C to a constant weight, recorded using a four-digit scale (SARTORIUS Model BT 224S). The sCOD of each sample was evaluated colorimetrically following the 5220 D standard method of the American Society for Testing and Material (ASTM).

The CFD model

The continuity equation of the three-phase flow CFD simulation in the AFFR was given by Eq. (1);

$$\frac{\partial\left(\rho_k\alpha_k\right)}{\partial t}+\nabla\cdot\left(\rho_k\alpha_k\vec{u_k}\right)=0, \tag{1}$$

where ρ is the density, α is the volume fraction, t is the time and $\vec{u}$ is the velocity vector. The subscript k can be replaced by l, g and s to denote the liquid, gas and solid phases, respectively.

The equation of motion for each phase [10-12] is then given by Eqs. (2) – (4):

The continuous phase:

$$\alpha_l\rho_l\frac{\partial\left(\vec{u_l}\right)}{\partial t}+\nabla(\rho_l\alpha_l\vec{u_l}\vec{u_l})=-\alpha_l\nabla p+\nabla\cdot\left(\alpha_l\mu_{eff,l}\left(\nabla\vec{u_l}+\left(\nabla\vec{u_l}\right)^T\right)\right)+\alpha_l\rho_l g+M_{lg}+M_{ls}, \tag{2}$$

The dispersed gas phase:

$$\alpha_g\rho_g\frac{\partial\left(\vec{u_g}\right)}{\partial t}+\nabla(\rho_g\alpha_g\vec{u_g}\vec{u_g})=-\alpha_g\nabla p+\nabla\cdot\left(\alpha_g\mu_{eff,g}\left(\nabla\vec{u_g}+\left(\nabla\vec{u_g}\right)^T\right)\right)+\alpha_g\rho_g g-M_{lg}, \tag{3}$$

The dispersed solid phase:

$$\alpha_s \rho_s \frac{\partial\left(\overrightarrow{u_s}\right)}{\partial t} + \nabla(\rho_s \alpha_s \overrightarrow{u_s}\overrightarrow{u_s}) = -\alpha_s \nabla p + \nabla \cdot \left(\alpha_s \mu_{eff,s} \left(\nabla \overrightarrow{u_s} + \left(\nabla \overrightarrow{u_s} \right)^T \right) \right) + \alpha_s \rho_s g - M_{ls}, \quad (4)$$

where p is the system's pressure, g is the gravitational force, μ_{eff} is the effective viscosity and M_{lg} and M_{ls} are the forces exerted on the continuous phase by the dispersed gas and solid phases, respectively.

Interphase momentum transfer

The drag force exerted on the liquid phase can be calculated from Eq. (5) [10,12]:

$$M_{1j} = C_{D,1j} \frac{3}{4} \rho_l \frac{\alpha_j}{d_j} \left| \vec{u}_j - \vec{u}_l \right| \left(\vec{u}_j - \vec{u}_l \right), \quad (5)$$

where $C_{D,lj}$ is the drag coefficient. The subscript j can be replaced by g and s to denote the gas and solid phases, respectively.

The gas phase was considered as sparsely distributed particles in the model, because of the low volume fraction. The drag coefficient between a liquid and gas phase is given in Eq. (6) following the Schiller Naumann drag model [13,14]:

$$C_{D,lg} = Max\left\{ \frac{24}{Re_g}\left(1 + 0.15\, Re_g^{0.687}\right), 0.44 \right\}, \quad (6)$$

where the solid particle Reynolds' number was in the inertia regime, the drag coefficient between the liquid and solid phase ($C_{D,ls}$) is 0.44 and Re_g is the relative Reynolds' number of the gas phase, which is given by Eq. (7);

$$Re_g = \frac{\rho_l d_g \left| \vec{u}_l - \vec{u}_g \right|}{\mu_l}, \quad (7)$$

where μ_l is the solid particle

Turbulence closure

The standard two-equation k-ε turbulent model was used for simulating the turbulence kinetic energy and its dissipation. The simulation of a multiphase turbulent flow is computationally expensive due to the influence of the dispersed phases on the continuous phase's turbulence [12]. The simulation was, therefore, considered as a multiphase flow with dilute dispersed phases. This assumption segregated the k-ε partial differential

equations to be solved only for the primary continuous phase. The turbulences of the diluted dispersed phases, which occupied a volume fraction of 0.18, were simulated by relating their kinematic viscosities with that of the continuous phase, named the dispersed phase zero equation approach [10].

The effective viscosity was obtained from Eq. (8) [15];

$$\mu_{eff,k} = \mu_k + \mu_{t,k}, \tag{8}$$

where μ_k and $\mu_{t,k}$ are the kinematic and turbulent viscosities, respectively, of phase k.

The turbulent viscosity of the continuous phase is given by Eq. (9) [10,12];

$$\mu_{t,l} = c_\mu \rho_l \left(\frac{k_l^2}{\varepsilon_l} \right), \tag{9}$$

where c_μ = 0.09, k is the turbulence kinetic energy and ε is the turbulence kinetic energy dissipation.

The turbulence kinetic energy and the turbulence kinetic energy dissipation can be calculated from Eqs. (10) and (11), respectively [10,12,15,16]:

$$\frac{\partial}{\partial t}\left(\alpha_l \rho_l k_l\right) + \nabla \cdot \left(\alpha_l \left(\rho_l \vec{u} k_l - \left(\mu + \frac{\mu_{t,l}}{\sigma_k} \right) \nabla k_l \right) \right) = \alpha_l \left(P_l - \rho_l \varepsilon_l \right), \tag{10}$$

$$\frac{\partial}{\partial t}\left(\alpha_l \rho_l \varepsilon_l\right) + \nabla \cdot \left(\alpha_l \rho_l u_{\max,l} \varepsilon_l - \left(\mu + \frac{\mu_{t,l}}{\sigma_\varepsilon} \right) \nabla \varepsilon_l \right) = \alpha_l \frac{\varepsilon_l}{k_l} \left(C_{\varepsilon 1} P_l - C_{\varepsilon 2} \rho_l \varepsilon_l \right), \tag{11}$$

where $u_{max,l}$ is the maximum velocity of the liquid domain and the constants $C_{\varepsilon 1}$, $C_{\varepsilon 2}$, σ_k and σ_ε were 1.44, 1.92, 1.0 and 1.3, respectively.

The relationship between the turbulent viscosity in the continuous and dispersed phases is given by Eqs. (12) and (13), respectively, [10]:

$$\mu_{t,g} = \frac{\rho_g}{\rho_l} \mu_{t,l}, \tag{12}$$

$$\mu_{t,s} = \frac{\rho_s}{\rho_l} \mu_{t,l}. \tag{13}$$

Upflow AFFR for wastewater treatment model

The AFFR model was created by Gambit 2.4.6®, with identical geometry to the cassava starch factory AFFR, as shown in Figure 2. The model was setup in Cartesian coordinates with the height (6 m) aligned on the z-coordinate while the x- and y-coordinates were the radial distance. The media was installed covering the reactor's height from 1–5 m. Three-phase flow simulation was performed by CFD using an Eulerian-Eulerian approach and the flow behavior of each phase was simulated as individual continua [10-12]. The volume of the anaerobic upflow reactor model was discretized by a tetrahedral mesh, with an optimal resolution of 5, 918, 123. The momentum conservation equation and interface drag models based on Ruttithiwapanich *et al*. [17] were applied. The model was simulated under atmospheric pressure, without heat and mass transfer. The fluid was assumed to be Newtonian, incompressible and fully developed and assumed a no-slip condition for the wall and liquid and a free-slip condition for the gas and solid phases. The sludge bed was simplified to that no biogas accumulated inside the sludge while the produced biogas was emulated by the input of gas from the reactor bottom since the biogas bubbles are mainly produced in the sludge bed zone. The upper surface of the model was a free surface and allowed only gas to exit. The solid sludge particles were set at a constant 2 mm diameter. Likewise, in this study, the size of the gas bubbles was set at 1 mm diameter, which was based upon the observed size of biogas bubbles leaving the sludge bed in a 5.5 L lab-scale AUR. The effect of changes in the bubble diameter on the biogas aggregation and segregation will be evaluated in a later study. The initial condition of the simulation and parameters are shown in Table 1.

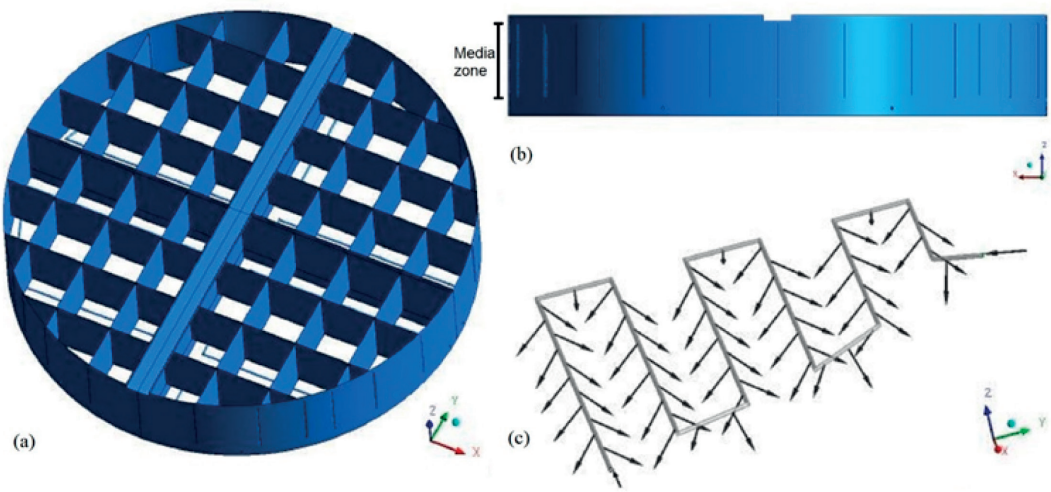

Figure 2 Scheme of the AFFR model showing the (a) isometric view, (b) side view and (c) inlet distribution pipe at the reactor's bottom.

Table 1 Model boundary conditions and parameters

Description	Values
Liquid phase	Liquid water at 25°C
Solid phase	Granular sludge, density of 1,024 kg/m^3 [18]
Gas phase	Air at 25°C
Reactor working volume	4,750 m^3
Inlet boundary condition	Velocity inlet, feeding flowrate of 1,200 m^3/d
Outlet boundary condition	Outlet
Wall boundary condition	No slip for liquid, free slip for solid and gas
Initial solid volume fraction	0.18
Initial gas volume fraction	0
Liquid-Solid momentum transfer	Drag coefficient = 0.44
Liquid-Gas momentum transfer	Schiller Naumann drag model
Reference operating pressure [atm]	1
Inlet concentration	20,000 mg COD/L
COD removal efficiency	90% COD removal
Biogas production yield	0.5 m^3/kg COD removal

Due to the symmetric character of the reactor, only a quarter of the reactor's volume was simulated. The CFD software package ANSYS CFX 12.0 was used for simulation with the terminating condition set as 1% for the domain imbalance and 10^{-4} for the root mean square (RMS) error. A computer with 64-bit dual processors of Intel Xeon E5-2620 @ 2.00 GHz and 32 GB RAM was used to run the package.

3. RESULTS AND DISCUSSION

Solid and substrate distribution inside the AFFR

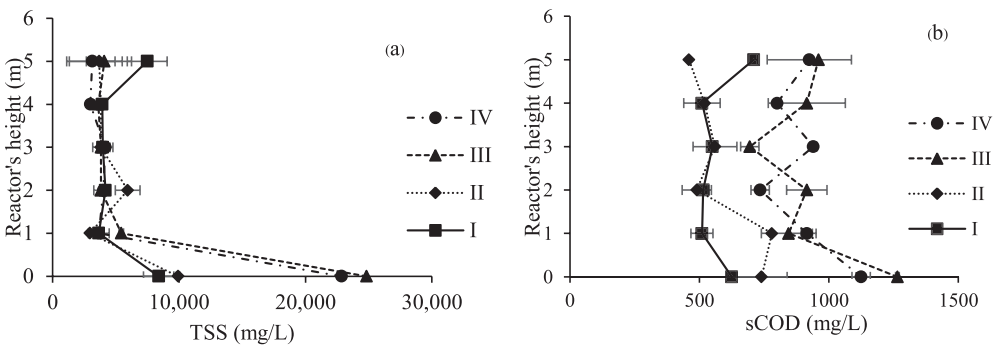

Figure 3 Profile of the (a) TSS and (b) sCOD along the AFFR height.

The solid distribution inside the AFFR was inhomogeneous, as shown in Figure 3a. The granular sludge concentration was lower in quarters I and II, with a maximum and minimum TSS of 8,393.3 ± 1,579.2 mg/L and 3,671.7 ± 134.4 mg/L, respectively. The sludge accumulated in quarters III and IV with a TSS of 24,833.3 ± 1,414.2 mg/L and 3,125.0 ± 176.8 mg/L, respectively. In all four quarters, the sludge concentration profiles were higher at the reactor bottom, which was the sludge bed area. The effect of media packing on the granular sludge distribution can be seen at a reactor height between 1–4 m. The sludge concentration sharply reduced at a reactor height of 1 m because the media resisted the liquid upflow velocity, as discussed in the next section. The sCOD profile is shown in Figure 3b, where the sCOD in quarters I and II were low at all reactor heights with a maximum and the minimum sCOD of 780.0 mg/L and 460.0 mg/L, respectively, in quarter II and 710.0 ± 14.1 mg/L and 501.0 ± 42.4 mg/L, respectively, in quarter I. The sCOD profile in quarter I remained lowest at all reactor heights (except for 5 m) because the upflow wastewater passed through this zone and the microbial activity degrading the organic substances in wastewater had a high activity in this area. The accumulation of organic substances was found in reactor quarters II, III and IV, where the sCOD was higher at the reactor bottom because of the inlet distribution zone, and lower in the upper portion of the reactor.

Three-phase flow pattern inside the AFFR

The liquid flow pattern in the AFFR is shown in Figure 4. The installation of the media for biofilm attachment created 15 zones in the liquid upflow structures in each reactor quarter. A water back-flow pattern, from the reactor top to the bottom, appeared all over the reactor because of the outlet weir that was located in the middle of the reactor. Wastewater in the area located away from the weir flowed downwards because of gravity, before reaching the outlet.This mechanism enhanced the mixing degree of the wastewater between the reactor top and the bottom.

The liquid upflow velocity is shown in Figure 5, including the area of a high liquid upflow velocity that appeared beneath the fixed film zone. The momentum of the inlet injection, together with the gas bubbles escaping from the bed, enhanced the liquid upflow velocity surrounding the inlet distribution pipe [19], as shown in Figure 6a. The liquid upflow velocity at the middle height of the sludge bed (0.5 m) was driven by the gas bubbles, where the average liquid upflow velocity (0.0511 m/s) was close to the gas bubbling velocity (0.057 m/s). By eliminating the gas bubbling effect, the two-phase simulation between liquid and solid revealed an average liquid upflow velocity in the same area was only 0.020 m/s. Thus, the gas bubbling mechanism enhanced the liquid upflow velocity [8]. The highest liquid upflow velocity appeared in the sludge bed because of the Venturi effect, where the liquid velocity increases when flowing through the small channels among the sludge granules [20,21].

The granular sludge was mainly packed on the reactor floor (Figure 6b) because the liquid upflow velocity in the upper zone of the reactor was lower than the sludge's terminal velocity (0.0276 m/s). The drag force at this condition was not enough to keep the granular sludge floating.

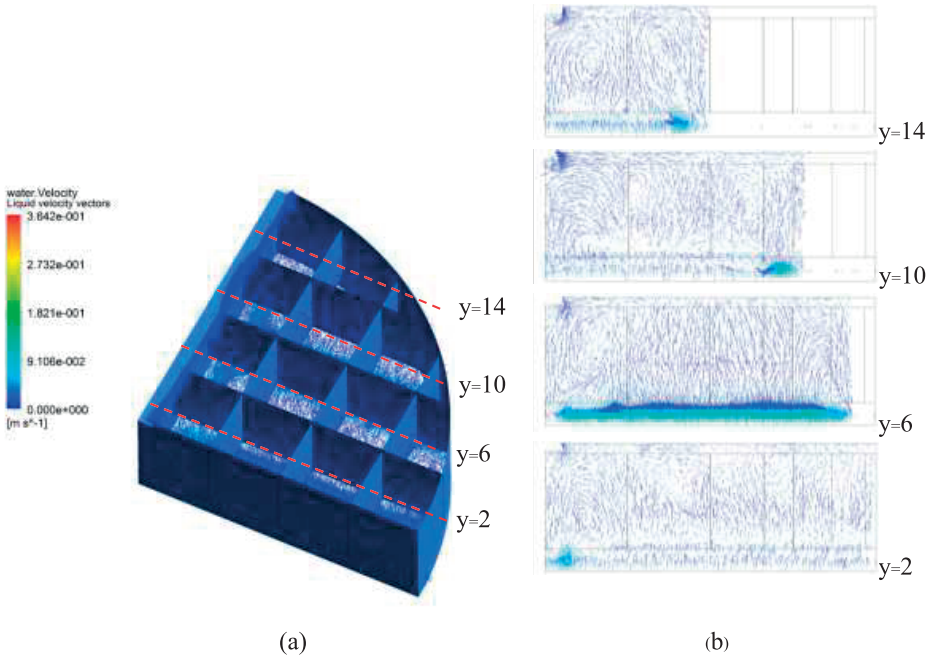

Figure 4 The liquid phase velocity vectors in a quarter of the industrial-scale AFFR model showing the (a) isometric-view and (b) velocity vectors on the xz-plane at y = 2, 6, 10 and 14 m.

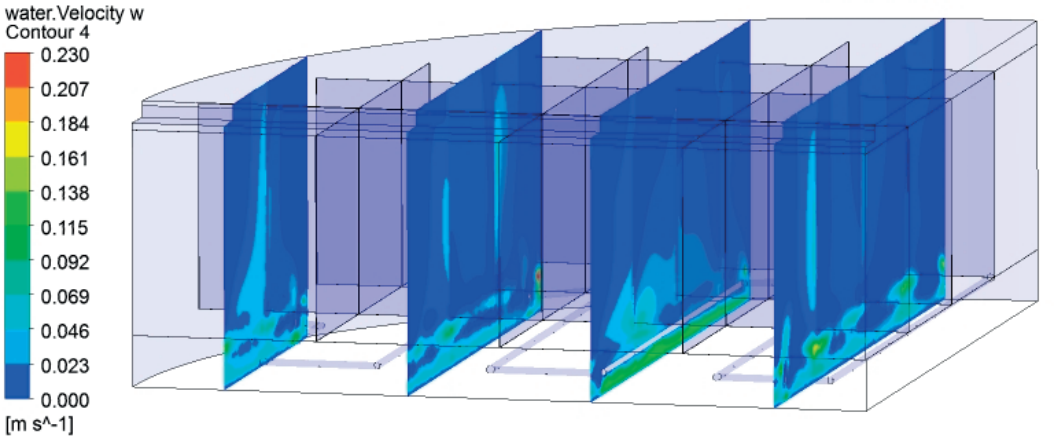

Figure 5 The liquid upflow velocity contours in a quarter of the AFFR model, on the xz-plane at y = 2, 6, 10 and 14.

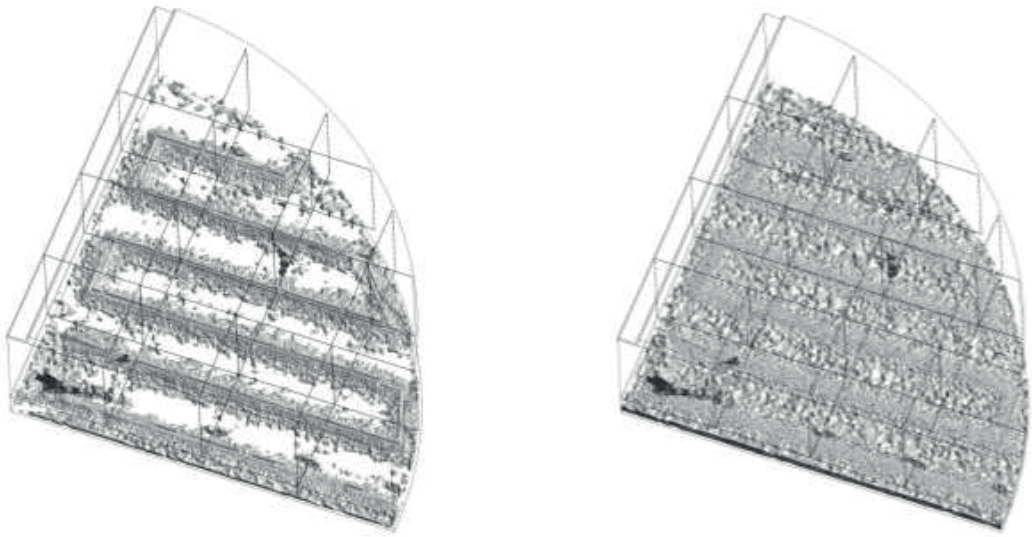

Figure 6 The iso-volume showing the area of the (a) liquid upflow velocity that was higher than the terminal velocity of the sludge (0.0276 m/s) and (b) solid/node volume fraction above 0.269.

The CFD simulation also showed the inlet nozzles nearby the reactor wall accelerated the wastewater upflow velocity. As the nozzles injected inlet wastewater at an angle of 45° downwards to the reactor floor, this injection encouraged the inlet water-wall collision, as shown in Figure 7. The collision shifted the liquid radial momentum transfer to be axial. Wastewater upflow with a velocity higher than the terminal velocity of the granular sludge (0.0276 m/s) was found at the regions adjacent to the reactor wall. This area provided a preferential channel for the granular sludge floating from the reactor bottom to the reactor top. After 15 y of reactor operation, the thickening of the biofilm together with the floating granular sludge could block the media packing zone [22] and caused the inhomogeneous TSS and sCOD profiles. It was previously found that using a horizontal inlet orifice nearby to the reactor's wall reduced both the axial momentum transfer andthe granular sludge washout [22]. Thus, a properly designed the inlet orifice can be the way to optimize the liquid-granular sludge momentum transfer to increase granular sludge flotation and enhance the mixing between the inlet wastewater and sludge.

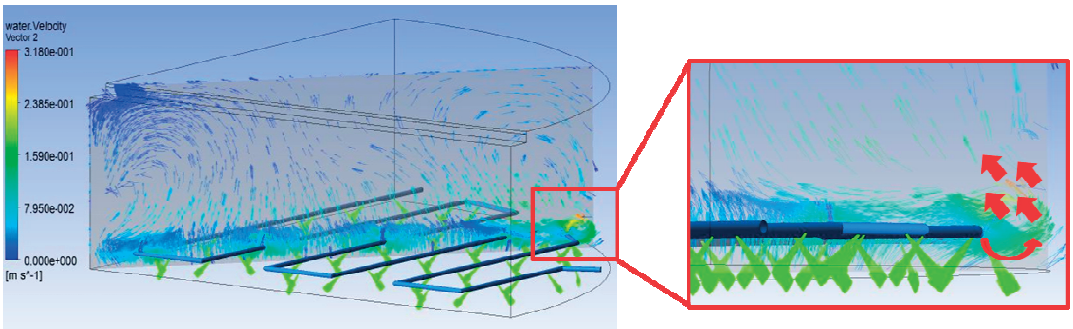

Figure 7 The inlet nozzles with a 45° angle downwards to the reactor floor, which encourages the collision between the inlet wastewater and the reactor wall.

4. CONCLUSIONS

The granular sludge and substrate distribution in the cassava starch factory AFFR was inhomogeneous. The higher degree of mixing in reactor quarters I and II was beneficial for the microbial activity, as reflected by the lower sCOD profiles in quarters I and II than in quarters III and IV. The improper inlet design over-accelerated the water upflow velocity, particularly in the areas nearby the wall. Areas of high water upflow velocity created channels for granular sludge washout. A horizontal inlet orifice is one option for optimizing the liquid-granular sludge momentum transfer.

5. ACKNOWLEDGMENTS

The authors gratefully acknowledge the financial support from the Thailand Research Fund through the Royal Golden Jubilee Ph.D. Program (Grant No. PHD/0121/2551). The Pilot Plant Development and Training Institute: PDTI and Choncharoen Co., Ltd are also acknowledged for supporting the research area.

6. REFERENCES

1. Suwanasri, K., Trakulvichean, S., Grudloyma, U., Songkasiri, W., Commins, T., Chaiprasert, P. and Tanticharoen, M., 2015, "Biogas – Key Success Factors for Promotion in Thailand," *Journal of Sustainable Energy and Environment Special Issue*, pp. 25-30.

2. Kullavanijaya, P. Paepatung, N., Laopitinun, O., Nopharatana, A., Chaiprasert, P. and Songaksiri, W., 2006, "An Overview of Status and Potential of Biomethanation Technology in Thailand," *KMUTT Research and Development Journal*, 30 (4),pp. 693-700.

3. Bhunia, P. and Ghangrekar, M.M., 2008, "Influence of Biogas-induced Mixing on Granulation in UASB Reactors," *Biochemical Engineering Journal*, 41, pp. 136–141.

4. Chapman, D., 1989, "Mixing in Anaerobic Digesters : State of the Art," pp. 325-354, in P. Cheremisinoff (Ed.) *Encyclopedia of Environmental Control Technology*, Vol. 3, Gulf Publishing, Houston.

5. McMahon, K.D., Stroot, P.G., Mackie, I.R. and Raskin, L., 2001, "Anaerobic Co-digestion of Municipal Solid Waste and Biosolids under Various Mixing Conditions - II Microbial Population Dynamics," *Water Research*, 35 (7), pp. 1817-1827.

6. Stroot, P.G., McMahon, K.D., Mackie, R.I. and Raskin, L., 2001, "Anaerobic Codigestion of Municipal

Solid Waste and Biosolids under Various Mixing Conditions-I. Digester Performance," *Water Research*, 35 (7), pp. 1804–1816.

7. Karim, K., Hoffmann, R., Klasson, T. and Dahhan, A.I., 2005, "Anaerobic Digestion of Animal Waste : Waste Strength Versus Impact of Mixing," *Bioresource Technology*, 96, pp. 1771-1781.

8. Smith, L.C., Elliot, D. J. and James, A., 1996, "Mixing in Upflow Anaerobic Filters and its Influence on Performance and Scale-up," *Water Research*, 30 (12), pp. 3061-307.

9. Cheng, Y., Wei, F., Yang, G. and Jin, Y., 1998, "Inlet and Outlet Effects on Flow Patterns in Gas-solid Risers," *Powder Technology*, 98, pp. 151-156.

10. Panneerselvam, R., Savithri, S. and Surender, G.D., 2009, "CFD Simulation of Hydrodynamics of Gas–liquid–solid Fluidised Bed Reactor," *Chemical Engineering Science*, 64, pp. 1119-1135.

11. Murthy, B.N., Ghadge, R.S. and Joshi, J.B., 2007, "CFD Simulations of Gas–liquid–solid Stirred Reactor : Prediction of Critical Impeller Speed for Solid Suspension," *Chemical Engineering Science*, 62, pp. 7184–7195.

12. Wang, X., Jie, D., Ren, N. Q., Liu, B.F. and Guo, W. Q., 2009, "CFD Simulation of an Expanded Granular Sludge Bed (EGSB) Reactor for Biohydrogen Production," *International Journal of Hydrogen Energy*, 34, pp. 9686-9695.

13. Schiller, L. and Naumann, A., 1935, "A Drag Coefficient Correlation," *Zeitschrift des Vereins Deutscher Ingenieure*, 77, pp. 318-320.

14. Yuxian, H., Weiyao, Z. and Yabing, G., 2010, "Numerical Simulation of Gas-liquid Flow in Plug Flow Aeration Tanks," *2010 4th International Conference on Bioinformatics and Biomedical Engineering*, Chengdu, China.

15. Diaz, M.E., Iranzo, A., Cuadra, D., Barbero, R., Montes, F.J. and Galan, M.A., 2008, "Numerical Simulation of the Gas–liquid Flow in a Laboratory Scale Bubble Column: Influence of Bubble Size Distribution and Non-drag Forces," *Chemical Engineering Journal*, 139, pp. 363-379.

16. Li, G., Yang, X. and Dai, G., 2009, "CFD Simulation of Effects of the Configuration of Gas Distributors on Gas–liquid Flow and Mixing in a Bubble Column," *Chemical Engineering Science*, 64, pp. 5104–5116.

17. Ruttithiwapanich, T., Ruenglertpanyakul, W. and Songkasiri, W., 2013, "Identification of Granular Sludge Wash-out origin Inside an Upflow Industrial-scale Biogas Reactor by the Three-phase Flow Model," *International Conference on Agricultural and Natural Resources Engineering*, 1-2 May 2013, Singapore.

18. Khankruer, D., 2002, Effect of Upflow Velocity on Granalation in UASB Treating Carbohydrate Wastewater, King Mongkut's University of Technology Thonburi, Bangkok, pp. 69-109.

19. Narnoli, S.K. and Mehrotra, I., 1996, "Sludge Blanket of UASB Reactor: Mathematical Simulation," *Water Research*, 31 (4), pp. 715-726.

20. Gomez, R.R., 2011, Upflow Anaerobic Sludge Blanket Reactor: Modelling, Licentiate Thesis, Royal Institute of Technology, pp. 16-18.

21. Atmakidis, T. and Kenig, Y.E., 2009, "A Numerical Study on the Residence Time Distribution in Low and Moderate Tube/particle Diameter Ratio Fixed Bed Reactor," *Chemical Engineering Transactions*, 18, pp. 1-6.

22. Escudie, R., Conte, T., Steyer, J.P. and Delgenes, J.P., 2005, "Hydrodynamic and Biokinetic Models of an Anaerobic Fixed-bed Reactor," *Process Biochemistry,* 40, pp. 2311-2323.